Identifying coherent patterns of environmental change between multiple, multivariate records: an application to four 1000-year diatom records from Victoria, Australia

Jonathan Tyler[1,2,3*], Keely Mills[2,4,5], Cameron Barr[6], Kale Sniderman[1], Peter Gell[2] and David Karoly[1]

[1]School of Earth Sciences, University of Melbourne;

[2]Water Research Network, Federation University, Australia;

[3]Department of Earth Sciences, University of Adelaide;

[4]British Geological Survey, Keyworth, Nottingham;

[5]Department of Geography, Loughborough University;

[6]School of Geography, Environment and Population, University of Adelaide.

* corresponding author: jonathan.tyler@adelaide.edu.au

Abstract

Empirical orthogonal functions (EOFs) of indirect archives of environmental change are increasingly used to identify coherent trends between palaeoclimate records, to separate externally forced patterns from locally driven idiosyncrasies. Lake sediments are particularly suited to such syntheses: they are abundant in most landscapes and record a wide array of information, yet local complexities often conceal or confuse the climate signal recorded at individual sites. Lake sediment parameters usually exhibit non-linear, multivariate and indirect responses to climate, therefore identifying coherent patterns between two or more lake records presents a complex challenge. Ideally, the selection of representative variables should be non-subjective and inclusive of as many different variables as possible, allowing for unexpected correlations between sites. In order to meet such demands, we propose a two-tier ordination procedure whereby site-specific (local) ordinations, obtained using Detrended

Correspondence Analysis (DCA), are nested within a second, regional EOF. Using the local DCAs as representative variables allows the retention of a larger fraction of variance from each site, removes any subjectivity from variable selection and retains the potential for observing multiple, coherent signals from within and between each dataset. We explore this potential using four decadally resolved diatom records from volcanic lakes in Western Victoria, Australia. The records span the 1000 years prior to European settlement in CE 1803. Our analyses reveal at least two coherent patterns of ecological change that are manifest in each of the four datasets, patterns which may have been overlooked by a single-variable, empirical orthogonal function approach. This intra-site coherency provides a valuable step towards understanding multi-decadal hydroclimate variability in southeastern Australia.

Introduction

Our understanding of Southern Hemispheric climate variability on multi-decadal to multi-centennial timescales is limited by a scarcity of quantitative, sub-decadally resolved climate records, a problem which is particularly manifest in Australia. To date there are only three annually resolved palaeoclimate records from Australia which extend further back in time than the most recent c. 350 years, and those are located in the latitudinal extremes of Tasmania and the northern tropics (Cook et al., 2000; Haig et al., 2014; Neukom and Gergis, 2012; PAGES 2k Consortium, 2013). By contrast, a number of sedimentary records exist, from shallow coastal/marine areas, lakes, peat bogs and speleothems, some of which span multiple millennia at sub-decadal resolution, but limited by some degree of chronological uncertainty *(Barr et al., 2014; Dodson et al., 1994; Mills et al., 2013; Mooney, 1997; Saunders et al., 2013; Saunders et al., 2012; Wilkins et al., 2013)*. In most cases, these archives offer indirect records of climate change, via geochemical, sedimentological and palaeoecological properties, limiting the potential for deriving quantitative climate records. However, identification of coherent patterns amongst multiple datasets can provide

52 convincing evidence for regional scale climate or hydrological change. Importantly, by
53 combining datasets, it is possible to separate patterns of externally forced climate variability
54 from the idiosyncrasies which may exist within stand-alone records. Such potential has been
55 highlighted by the use of empirical orthogonal functions (EOFs), derived using principal
56 components analysis (PCA), in order to identify the coherent patterns between multiple
57 records within regional and global palaeoclimate datasets (Anchukaitis and Tierney, 2012;
58 Clark et al., 2009; Clark et al., 2007; Clark et al., 2012; Shakun and Carlson, 2010; Shakun et
59 al., 2012; Tierney et al., 2013).

60 The use of EOFs is well grounded in climate and palaeoclimate research, but the majority of
61 studies have applied the technique to either instrumental data or annually resolved
62 palaeoclimate records such as tree ring or coral datasets (Mann et al., 1998; Smith et al.,
63 1996; Weare et al., 1976). The extraction of EOFs from sedimentary archives represents a
64 particular challenge due to the uncertainties associated with both dating and climatic
65 interpretation. Recent implementation of Monte Carlo iterative age modelling within EOF
66 analyses represents a valuable step towards dealing with age uncertainty in sediment records
67 (Anchukaitis and Tierney, 2012; Shakun and Carlson, 2010). However, an ongoing issue with
68 sediment based EOFs relates to the multivariate nature of many sedimentary records. Most
69 sedimentary archives contain multiple lines of information, including geochemical
70 parameters, microfossil remains or sedimentological properties. In the usual absence of
71 quantitative palaeoclimate reconstructions (e.g. temperature, rainfall; *Saunders et al. 2012;*
72 *2013*), the selection of representative variables from each site remains a source of ambiguity.
73 It is impossible to include all of these variables within a regional ordination: doing so would
74 fail the criterion of data independence and potentially bias the analysis to the site which
75 contributes the most variables. However, selecting a single representative timeseries from
76 each site can be subjective and can undermine the explorative element of the analysis. In
77 addition, reducing a detailed matrix to a single variable leads to the loss of potentially

78 relevant information and discards the considerable effort and time invested in collecting the
79 data in the first place.

80 One particular consequence of reducing multivariate palaeoecological data to single variables
81 prior to EOF analysis is that it undermines the possibility of observing correlations between
82 secondary modes of variability at two or more sites, despite the intuitive likelihood of such
83 correlations existing. Lake ecosystems are subjected to a variety of external and internal
84 forces, which ultimately determine the expression of their sedimentary record (Battarbee,
85 2000; Mills et al., 2014; Smol et al., 2005; Wigdahl et al., 2014). Neighbouring lake systems
86 exhibit different sensitivities to external forcing: a hypothetical 'Site A' might respond
87 dramatically to changes in rainfall, through changes in lake level, whilst the effect of rainfall
88 upon 'Site B' might manifest in a more muted physical/ecological response, e.g. through
89 changing nutrient balance or lake water stratification. In such a scenario, even though rainfall
90 changes do affect 'Site B', a comparison of the major patterns of ecological change at both
91 sites would reveal limited coherency. Existing approaches to regional data syntheses do not
92 allow for such variable climate-lake interactions. We therefore propose an alternative
93 approach to exploring regional coherency between sedimentary archives using two-tiered
94 nested ordinations. This involves reducing each site-specific multivariate dataset to a series of
95 orthogonal variables using established methods of ecological data dimension reduction (in
96 this case, Detrended Correspondence Analysis; DCA). The DCA sample scores of all site
97 specific ordinations (hitherto termed 'local DCAs') are then combined within a 'regional'
98 (multiple site) EOF analysis, which is performed using PCA following previous studies. The
99 approach is applied to a suite of four diatom records from volcanic lakes in Western Victoria,
100 Australia, which span the millennium prior to European colonisation (CE 800 – 1800).
101 Coupled with iterative age modelling to account for age uncertainty similar to Anchukaitis
102 and Tierney (2012), our approach provides a flexible, multi-layered means of exploring
103 coherency between multivariate sediment records which allows for the detection of multiple
104 patterns of change.

105

106

107 **Sites and Methods**

108 Four sedimentary diatom records were selected from lakes within the western Victorian
109 Volcanic Plains, Australia. Those sites were Lake Purrumbete, Lake Elingamite, Lake
110 Surprise and Tower Hill Main Lake (Figure 1). Each of the lakes is situated in a late
111 Pleistocene volcanic crater, located within 50 km of the western coastline of Victoria. The
112 climate of this region is Mediterranean in character, with cool, wet winters and mild, dry
113 summers. The four study sites were selected based on their proximity to each other,
114 similarities in lake and catchment morphology and size and because for each site there is a
115 recently derived diatom record which spans the last >1200 years at decadal or sub-decadal
116 temporal resolution. Given the sparse distribution of high-resolution records for the entire
117 Australian continent, let alone the Southern Hemisphere, this collection of similar datasets
118 from western Victoria represents a significant palaeoclimate resource.

119 All datasets used in this study bar one have been published, and therefore collection of
120 sediment cores and subsequent diatom analyses are discussed in those papers and reports
121 (Barr, 2010; Barr et al., 2014; Mills et al., 2013). All raw diatom data are available via the
122 NOAA Palaeoclimatology Database (http://www.ncdc.noaa.gov/data-
123 access/paleoclimatology-data). The previous papers and reports describe the dating
124 techniques employed, using a combination of radiocarbon analysis (of plant macrofossils,
125 pollen extracts and acid resistant organic material), ^{210}Pb dating of recent sediments and the
126 use of exotic pollen horizons in comparison with the known age of local European
127 colonisation. In some cases, the original authors were led to reject certain anomalous
128 radiocarbon ages, and those decisions are mirrored here. For Lake Elingamite and Lake
129 Surprise, a radiocarbon age offset was estimated based on differences between ^{14}C and ^{210}Pb
130 dates in the upper sediments (480 ± 44 years and 424 ± 74 years respectively; *Barr et al.*

131 *2014*). These offsets, which are interpreted to reflect the influence of radiometrically old
132 groundwater derived carbon, are also used here for consistency.

133 Age-depth models were derived using the CLAM program in R (Blaauw, 2010). In order to
134 maintain a consistent approach throughout, each of the four age models was constructed using
135 smoothed spline interpolation, with a relatively rigid smoothing factor of 0.6 chosen as one
136 which adequately captures the distribution of age constraints for all sites. ^{14}C ages were
137 calibrated against the Southern Hemisphere ^{14}C master chronology (Hogg et al., 2013), with
138 age uncertainties based on 10,000 Monte Carlo iterations (Blaauw, 2010).

139 In an approach which largely follows Anchukaitis and Tierney (2012), palaeoenvironmental
140 timeseries were generated and analysed within an iterative age modelling framework to
141 address the imprecision of radiocarbon- based chronologies. For each of the 10,000 CLAM
142 derived site-specific age models, each dataset was linearly interpolated, resampled at 5 year
143 intervals and truncated to the period 1180-150 years before CE 1950 (calibrated years before
144 present, cal. B.P.). This time period was selected based on (a) the youngest age iteration for
145 the bottommost sample from Lake Surprise, the shortest of the records examined and (b) the
146 need to exclude all data affected by post-European land use change, which has had marked,
147 non-climatic influences on each of the lake sites studied (Barr et al., 2014; Mills et al., 2013).
148 The interpolation step in our analyses mirrors previous studies (Anchukaitis and Tierney,
149 2012; Shakun and Carlson, 2010), however we acknowledge that this is a suboptimal solution
150 due to the potential alteration of the inherent variance in the timeseries. Future studies should
151 consider more complex, computationally intensive modeling-based approaches which are
152 outside the scope of this paper. Interpolation and truncation were carried out prior to any
153 statistical analysis because doing so afterwards can result in biased ordination results,
154 including the introduction of correlations between axes which were initially (by design)
155 orthogonal. For each site, we therefore generated 10,000 different matrices, where the
156 columns represent diatom species and the rows represent five-year time intervals. Each value

157 within an individual matrix is an interpolated species count (expressed as a %), varying
158 according to the fitted age model and associated interpolation.

159 Site specific datasets were processed using detrended correspondence analysis (DCA; Hill,
160 1979; Hill and Gauch, 1980) upon each interpolated matrix to reduce the multi-dimensional
161 dataset to a lower-dimensional subset, free of internal correlations. We used DCA, over the
162 more commonly used principal components analysis (PCA), because PCA is not well suited
163 to palaeolimnological diatom data, which are non-linear, have a high beta diversity and which
164 contain a large percentage of zero observations (Birks et al., 2012; Legendre and Legendre,
165 1998; Minchin, 1987). Alternative ordination techniques for the treatment of non-linear
166 biological data were explored, including PCA with Hellinger transformation (PCA-H;
167 Legendre and Gallagher, 2001), correspondence analysis (CA; Greenacre, 1984) and non-
168 metric multidimensional scaling (nMDS; Clarke and Warwick, 2001; Kruskal, 1967;
169 Minchin, 1987). nMDS is probably the most robust method for the treatment of biological
170 data (Faith et al., 1987; Minchin, 1987), however in the *k* dimensional ordination maps
171 produced by nMDS, those *k* dimensions are not independent and thus nMDS can not be used
172 to extract independent orthogonal vectors that summarise patterns of ecological change (P.
173 Minchin and G.L. Simpson, pers. comm.). In addition, we observed that PCA-H and CA
174 produced artifactual biases within the ordinations (known as 'horseshoe' and 'arch' effects
175 respectively). We therefore concluded that DCA produces the most satisfactory ordinations
176 for our purpose. Although DCA is commonly used in ecology, it has been subjected to some
177 criticism. In DCA, the arch effect is removed by detrending in segments (Hill, 1979) which is
178 considered an inelegant, manipulative and potentially subjective solution (Legendre and
179 Gallagher, 2001). In addition, the chi-squared distance metric used in both CA and DCA has
180 been criticised as a poor approximation of ecological distance (Faith et al., 1987). With this in
181 mind, we verified our DCA ordinations against two-dimensional nMDS, and found that both
182 methods inferred similar relationships between samples. We are therefore satisfied that DCA
183 captured robust, ecologically significant patterns. DCA was performed using *decorana* within

184 VEGAN for R (Hill, 1979; Oksanen et al., 2008). Prior to analysis, the interpolated
185 percentage species data were first square-root transformed and rare species were
186 downweighted. nMDS was performed using *metaMDS* within VEGAN (Oksanen et al., 2008)
187 using Bray-Curtis similarity matrices (Faith et al., 1987). A qualitative comparison between
188 the DCA axes and previously reported diatom inferred conductivity (salinity) reconstructions
189 for each of these sites was facilitated by plotting smooth response surfaces in the ordination
190 diagrams. Response surfaces were based on Generalised Additive Modelling (GAM),
191 embedded within the *ordisurf* function within VEGAN (Oksanen et al., 2008).

192 Regional (multiple site) EOFs, which summarise the common patterns of variability within
193 the whole dataset (in this case, the first three DCA axis scores for all sites), were obtained by
194 PCA using *rda* within VEGAN (Oksanen et al., 2008). As with the local DCAs, regional PCA
195 was performed for each of the 10,000 iterated age models. Previous applications of PCA
196 using sedimentary data have required standardisation by subtracting the mean and setting the
197 standard deviation to unity (Anchukaitis and Tierney, 2012; Clark et al., 2007; Shakun and
198 Carlson, 2010), but in this case the use of local DCAs meant that no further data
199 standardisation was required. Different iterations generated regional EOFs of alternating sign,
200 however because the sign of an EOF is irrelevant, all regional EOF iterations were screened
201 for correlation, and those which were inversely correlated to the first iteration were multiplied
202 by –1. For each of the local DCAs, and for the regional EOFs, the 68% and 90% confidence
203 intervals were calculated, which serve to provide error estimates associated with uncertainties
204 in age model determination. The number of significant EOFs was screened by comparing a
205 screeplot of variance explained with a random distribution based upon a broken stick model,
206 following Bennett (1996).

207

208 **Results**

209 Age-depth models (Figure 2) mirror those published elsewhere (Barr et al., 2014; Mills et al.,
210 2013). Lake Elingamite and Lake Surprise both have >5 radiocarbon age constraints younger
211 than 1500 cal. B.P., although both datasets are associated with large uncertainty around the
212 initial age determinations (Figure 2). Lake Purrumbete and Tower Hill Main Lake have only
213 three radiocarbon dates, spaced at ~2000 and ~1000 years respectively. These ^{14}C
214 measurements have smaller uncertainties, and both sets of dates are consistently
215 stratigraphically ordered. However the paucity of age constraints younger than 1000 cal. B.P.
216 is undoubtedly a source of potential error.

217 DCA biplots (Figure 3) depict the most common species associated with major modes of
218 ecological change at each site. For three of the sites, only taxa with a maximum abundance
219 ≥5% in at least one sample are displayed in order to reduce the number of taxa to around 10.
220 This cutoff was not feasible for Lake Surprise, which has 29 taxa with a maximum abundance
221 >5%, and 23 taxa with a maximum abundance >10% (as plotted in Figure 3c). This large
222 number of occasionally dominant taxa at Lake Surprise indicates a large degree of species
223 turnover and ecological instability. A more detailed discussion of the diatom species
224 composition of each sediment core can be found elsewhere (Barr, 2010; Barr et al., 2014;
225 Mills et al., 2013). For Lakes Tower Hill and Purrumbete, the first two DCA axes correlate
226 with diatom-inferred conductivity (Figures 3b and 3d). However for Lake Elingamite (Figure
227 3a), and particularly for Lake Surprise, the relationship is more complex, whereby high
228 conductivity estimates are associated with both positive and negative scores on both DCA
229 axes (Figure 3c).

230 Visual examination of the site specific DCA axes, plotted in time, reveals similar patterns
231 between sites (Figure 4), some of which are statistically significant correlations. In particular,
232 DCA 1 from both Tower Hill and Elingamite and DCA 2 from Purrumbete correlate ($r > 0.5$
233 or $r < –0.5$, based on mean values) (Figure 4). These three local DCAs exhibit a pattern of
234 increasing (decreasing) values between 1200-700 cal. B.P. and decreasing (increasing) values
235 between c. 700-200 cal. B.P. (Figure 4). By contrast, DCA 1 from Purrumbete and Surprise,

DCA 2 from Tower Hill and DCA 3 from Elingamite all exhibit long term trends of decreasing (increasing) values between 1200-200 cal. B.P. (Figure 4). DCA 3 from Purrumbete and Tower Hill exhibit clear variability over shorter (centennial-bicentennial) timescales, yet they do not appear to directly match up – a comparison which is not aided by the age uncertainties in these records (Figure 4).

Principal components analysis identifies two regional EOFs which explain a significant proportion of the variance within the local EOFs, assessed using the broken stick approach (Figure 5). Of the total variance, regional EOF 1 explains a mean of 27% and regional EOF 2 axis explains a mean 21%, with a cumulative sum of 48%. Such values are comparable to similar studies from other regions (e.g. Anchukaitis and Tierney, 2012).

The temporal patterns in regional EOFs 1 and 2 are also consistent with the qualitative assessment of their constituent local DCAs (Figure 6a). Regional EOF 1 exhibits a gradual increase between 1200-600 cal. B.P. followed by a slight decrease between 500-200 cal. B.P. (Figure 6a). This pattern best corresponds with local DCA 1 from Lake Purrumbete, although many of the other local DCAs also exhibit substantial positive or negative loading upon this axis (Figure 7). The suggestion is that EOF 1 captures a long term trend which is a consistent feature of all datasets. Regional EOF 2 exhibits a decrease between 1200-700 cal. B.P. and an increase between 700-400 cal. B.P. (Figure 6a). This pattern corresponds well with Tower Hill DCA 1, Purrumbete DCA 2, Elingamite DCA 1 and Surprise DCA 1 – i.e. it appears to be representative of the primary pattern of ecological change at three of the four sites (Figure 7).

Discussion

Methodological Considerations

Multi-site data syntheses are becoming an increasingly common feature of palaeoclimate research, providing both a means of exploring large datasets for coherent signals (Anchukaitis and Tierney, 2012; Clark et al., 2007; Nicholson et al., 2013; Shakun and Carlson, 2010) and of testing hypotheses on the nature of and controls behind global scale climate changes (Clark et al., 2009; Shakun et al., 2012; Tierney et al., 2013). The Monte Carlo Empirical Orthogonal Function of Anchukaitis and Tierney (2012) is a particularly useful methodological development, allowing for rigorous comparison of palaeoclimate timeseries within the age errors inherent to all sedimentary archives. However, despite such advances, uncertainties remain concerning the selection of variables for inclusion in such syntheses, which in the most part remains a largely subjective process. For example, the Anchukaitis and Tierney (2012) synthesis of East African palaeoclimate records involved a range of data types, including varve thickness, percentage of benthic diatom species, magnetic susceptibility and calcite Mg/Ca ratios. Although each of these variables can be qualitatively attributed to local hydrology or climate, none have been calibrated against a particular climate variable, the sensitivity of a those variables to climate change may vary geographically or through time and it is unclear to what extent they represent the overall patterns of environmental change at each site. Without having quantitative climate proxies to select, the need to limit multivariate datasets to a single variable, and the process of identifying which variable to use, represents a potentially major source of lost information.

In this study, our objective was to explore coherency between multiple multivariate datasets assuming no prior knowledge of each record, and with no *a priori* expectations for the pattern that would emerge. In response to the problem of selecting variables, we propose an alternative approach: to identify multiple representative signals from each site - obtained using local DCA analysis - and to include all of those signals within a regional EOF. The local DCAs produce a suite of independent variables and by retaining a larger amount of information, we retain the ability to explore multiple modes of variability between multiple sites. Performing DCA on each multivariate dataset removes any subjectivity related to data

287 selection, and with the objective to identify vectors which explain as much of the initial
288 variance as possible, the derived variables can be assumed to be representative of the
289 ecological patterns at each site. A similar approach was taken by Tierney et al. (2013),
290 whereby three variables from Lake Challa were reduced to a single local EOF 1 prior to
291 inclusion within the regional analysis, however in this case only hydrologically sensitive
292 variables were used and the lower order EOFs were not included in the final analysis.

293 All previous syntheses of sedimentary data have used PCA to derive EOFs, despite the fact
294 that PCA is poorly suited to the non-linearity of many data types, most notably
295 palaeoecological data (Birks et al., 2012; Jongman et al., 1987; Legendre and Legendre,
296 1998). Our two-tiered ordination approach allows the application of more appropriate
297 methods of ordination and transformation according to the nature of each specific dataset.
298 Amongst other benefits, performing ordination using each site specific dataset essentially
299 normalises the data to standard mean and variance, removing the requirement to undertake
300 any further data transformation prior to the multi-site analysis (cf. Emile-Geay and Tingley,
301 2014 - in press). In this study, we used detrended correspondence analysis (DCA) to process
302 each diatom microfossil dataset. DCA is well suited to biological datasets because it accounts
303 for the non-linearity of species-environment responses by assuming unimodal response curves
304 (Hill and Gauch, 1980). Our approach is also flexible to the possibility of including single
305 variable records (e.g. speleothem $\delta^{18}O$, tree ring width) for comparison with multivariate
306 datasets. In addition to PCA based EOFs of single variables, a number of techniques have
307 been employed to compare multivariate ecological datasets. For example, patterns of species
308 overturn between different organisms, or at different sites, have been traced using detrended
309 canonical correspondence analysis (Birks, 2007; Smol et al., 2005) or principal curves
310 analysis (Davidson et al., 2013; Simpson and Birks, 2012), whereas ordinations can be
311 compared directly using procrustes analysis (Chen et al., 2010; Davidson et al., 2007; Peres-
312 Neto and Jackson, 2001; Wischnewski et al., 2011a; Wischnewski et al., 2011b). However,
313 none of these methods result in the isolation of representative timeseries that summarise

coherent patterns of inter-site variability. In this respect, we consider PCA derived EOFs to be a sufficiently appropriate tool. By nesting local DCAs within a regional EOF, our approach is analogous to tree ring based palaeoclimatology, where densely sampled regional dendroclimatic data sets are represented by a smaller number of leading principal components in order to ensure that regions can be compared within a global network (e.g. Mann et al., 1998).

One source of uncertainty in our study relates to the imprecision of the age-depth models available for each core (Figure 2). Our treatment of age uncertainties is similar to that of Anchukaitis and Tierney (2012), but with some differences. For the sake of simplicity and consistency with other studies, we took the age-depth iterations directly from CLAM (Blaauw, 2010), which imparts no constraints other than rejecting age models which reverse with depth. This simple approach is considered parsimonious given the relatively few age constraints available for each site. However, in situations where more detailed age models are available, more sophisticated Bayesian based calibration tools could be implemented (e.g. Blaauw and Christen, 2011; Bronk Ramsey, 2008). Chronological imprecision likely has contrasting effects on the final EOFs extracted. On one hand, broad dating errors increase the likelihood of finding correlations between two timeseries, regardless of whether those correlations would exist in 'real' time. Certainly, two records which exhibit similar patterns but which are phase lagged will not be identified as such. On the other hand, if coherent and inherently linked patterns do occur between multiple records, an age iterated EOF approach will frequently identify them, essentially confirming visual impressions within the limits of chronological error. However, it is worth noting that the final EOF will ultimately converge upon an age model which reflects the individual record with the most precise chronology. In essence, this is not dissimilar to building age models based upon climate signal 'wiggle matching', a practice which is widely frowned upon in palaeoclimate research (Blaauw, 2012). As a consequence, no EOF should be interpreted in isolation from the original data,

with particular attention paid to the accuracy as well as precision of the age models concerned.

Interpretation of Diatom Patterns

The local DCA axes, by design, depict the major patterns of change within each diatom dataset (Table 1 and Figures 3 and 4). For each site, these local DCA axes primarily relate to hydrological change. One objective of this paper is to look beyond transfer function derived reconstructions, both due to limitations in understanding of the ecological preferences of diatoms within Australian wetlands and to problems with the use of transfer functions in general (Barr et al., 2014; Juggins, 2013). Nevertheless, the previously published conductivity (salinity) estimates for each of these sites provide a useful additional means of qualitatively interpreting the local DCA axes (Figure 3). At Lake Purrumbete and Lake Tower Hill, both local DCA axes correlate with diatom inferred conductivity, suggesting that hydroclimatic changes are a major source of variability in the diatom communities at these sites (Figures 3b and 3d). Lake Purrumbete has not undergone marked lake level change since European settlement (Leahy et al., 2010) and it has a sediment record which consists predominantly of planktonic and facultative planktonic diatoms (Table 1; Tibby et al., 2012). Diatom species changes at Lake Purrumbete most likely reflect changes in salinity, nutrient concentrations and physical limnology, factors which are indirectly affected by climate variability (Tibby and Tiller, 2007). DCA 2 from Lake Purrumbete is characterised by a shift from one group of deep water phytoplanktonic taxa, dominated by *Discostella pseudostelligera* and *Aulacoseira pusilla* to another dominated by *Discostella stelligera* (Table 1; Figure 3b). Similar shifts between these taxa have previously been attributed to changes in the degree of lake water mixing at Lake Purrumbete and elsewhere, whereby *Discostella stelligera* is more common in stratified waters (Tibby et al., 2012; Wang et al., 2008). Lake stratification is favoured by warm, dry conditions, which would also promote higher levels of salinity through lake water

366 evaporation. The diatom ecological changes associated with the major DCA axes at Tower
367 Hill are less tangible from a habitat perspective: the majority of taxa are benthic species with
368 either epiphytic, epipelic or facultative planktonic life strategies (e.g. *Sellaphora pupula*,
369 *Tabellaria fasiculata*, Table 1). At Tower Hill, it is feasible that changes in lake water salinity,
370 ionic composition, light attenuation or associated hydrological shifts were responsible for
371 changes in diatom species through time.

372 At Lake Elingamite, hydroclimatic change is clearly manifest as evidence for lake level
373 change, where the local DCA 1 depicts a shift between shallow water benthic or facultative
374 planktonic taxa (*Staurosirella construens* var. *construens*, *Staurosirella pinnata*,
375 *Psammothidium sacculum*) and deeper water, planktonic taxa (*Fragilaria crotonensis*,
376 *Discostella stelligera*, *Discostella pseudostelligera*) (Table 1; Figure 3a). It is therefore
377 reasonable to interpret the DCA 1 from Lake Elingamite as being a negative function of
378 changes in lake water depth and salinity, which in turn is influenced by changes in effective
379 moisture. The hydrological sensitivity of Lake Elingamite to climate variability is evident
380 from the lake level changes at this site during the last century (Barr, 2010; Barr et al., 2014).
381 For Lake Surprise, neither of the first two DCA axes consistently relate to diatom-inferred
382 conductivity (Figure 3c). DCA 1 exhibits both positive and negative association with
383 conductivity, depending on whether DCA 2 is either positive or negative (Figure 3c). The
384 major pattern in DCA 1 is a contrast between a group of predominantly benthic taxa
385 (*Achnanthidium minutissimum*, *Nitzschia palea* and *Encyonopsis ruttneri*) which associate
386 with positive DCA 1 values and a group of planktonic taxa (*Discostella stelligera,*
387 *Stephanodiscus hantzschii* and *Cyclostephanos dubius*) which associate with negative DCA 1
388 values (Table 1; Figure 3c). DCA 2 at Lake Surprise describes a contrast between two groups
389 of planktonic diatom taxa (*Discostella stelligera* and *Discostella pseudostelligera* vs.
390 *Stephanodiscus hantzschii* and *Cyclostephanos dubius*) which may relate to changes in water
391 chemistry or lake water stratification patterns (Table 1; Figure 3c).

392 The regional EOFs agree well with the individual local DCAs from which they are based
393 (Figures 6 and 7). It appears that regional EOF 1 traces a long term, 'background' signal which
394 is evident in most of the records, and the principle mode of change at Lake Purrumbete. By
395 contrast, regional EOF 2 illustrates the major mode of change at the other three sites, being
396 prominently expressed in DCA 1 from Tower Hill, Lake Elingamite and Lake Surprise, as
397 well as DCA 2 from Lake Purrumbete (Figure 6a). The results therefore suggest that each of
398 the four sites underwent ecological changes which followed similar trajectories and timing,
399 although not necessarily in the same manner. Common ecological trajectories need not be
400 climatically driven: they can occur in response to regional scale environmental changes, such
401 as land surface and lake ecosystem development following a geological event (e.g. volcanic
402 eruption) or major climate/environment rebound, as can be observed during the retraction of
403 deserts or following glacial retreat (Anderson et al., 2012; Engstrom et al., 2000). However,
404 given the sensitivity of these sites to hydrological change, and the further connection between
405 diatom taxa and hydrologically driven changes in lake water salinity and water depth, it is
406 reasonable to infer that the regionally coherent patterns of change relate to a common climate
407 forcing.

408

409 In addition to identifying common patterns of change amongst sites, there is potential with
410 our approach to identify and isolate the differences exhibited by individual sites relative to the
411 collective regional signal. This would provide a quantitative tool to explore the variable
412 responses of aquatic ecosystems to climate or other widespread environmental changes over
413 timescales of decades to millennia. Such analyses are beyond the scope of this paper, but they
414 might ideally utilise additional, quantitative palaeoclimate reconstructions as explanatory
415 variables and involve a detailed analysis of the site-specific factors (lake bathymetry,
416 catchment morphology, soil or vegetation composition, geographic position) that lead to
417 divergences in ecosystem response through time. Such a study would also facilitate a critique

418 of the validity of using a single lake sediment record as an archive of regional environmental
419 change, or identify the features of those lakes that are indeed sentinels of widespread patterns.

420

421 Environmental change in southeastern Australia during the last millennium

422 Ongoing and future data synthesis research aims to implement the approach outlined here, as
423 well as published alternatives, to integrate a range of palaeoclimate records from Australia
424 and its surrounding regions. In the interim, here we compare the Victorian diatom regional
425 EOFs with key palaeoclimate records from south-eastern Australia to qualitatively
426 demonstrate the consistency of our results within a regional climatic framework. Long term
427 records of environmental change in southeastern Australia suggest a progressive decline in
428 rainfall occurred since the mid-Holocene, culminating at ~2000 cal B.P., at which point Lake
429 Keilambete water depth was at its lowest, and Lake Tyrrell in inland Victoria completely
430 dried out (Bowler and Hamada, 1971; De Deckker, 1982; Gouramanis et al., 2013). More
431 recently, diatom-inferred salinity reconstructions from Lake Elingamite and Lake Surprise
432 indicate a marked period of low effective moisture occurred at ~1200 cal B.P. which was
433 followed by a progressive decrease in lake water salinity (increased effective moisture) until
434 ~150 cal B.P. (Barr et al., 2014). A similar pattern can be observed in the frequency of
435 carbonate laminae deposition in Lakes Keilambete and Gnotuk, Victoria (Figure 6b), which
436 can also be interpreted as reflecting a progressive increase in effective moisture during the
437 last millennium (Wilkins et al., 2012; Wilkins et al., 2013). These changes are consistent with
438 the patter of progressive change illustrated by regional EOF 1, which might reflect both an
439 increase in rainfall since ~2000 cal B.P. as well as a long term hydrological and ecological re-
440 equilibration following the prolonged period of low rainfall prior to the start of these records.

441 Regional EOF 2 can also be interpreted as a pattern of hydroclimate change which is manifest
442 as the major pattern of change at all sites except Lake Purrumbete (Figures 4 and 6a).
443 Referring back to the local DCA analyses suggests that EOF 2 is best interpreted as a positive

444 function of regional moisture balance, i.e. deeper, less saline lakes, reflecting either higher
445 rainfall, reduced evaporation or increased groundwater flow. The hydrological sensitivity of
446 EOF 2 is illustrated by the similarity with the low frequency component in diatom-inferred
447 conductivity from Lake Elingamite (Figure 6b). Other lakes in the region exhibit similar
448 patterns of change, most notably Blue Lake, Mt. Gambier, South Australia, whereby oxygen
449 isotope measurements from ostracods suggest an increase in evaporation relative to
450 precipitation between 1100-500 cal B.P., followed by a reversal of that trend between 500-
451 150 cal B.P. (Figure 6b; Gouramanis et al., 2010). A sediment pigment-inferred rainfall
452 reconstruction from Rebecca Lagoon in Tasmania also implies that the period prior to 500 cal
453 B.P. was relatively dry, followed by an increase in rainfall between 500-100 cal B.P. (Figure
454 6b; Saunders et al., 2012).

455 In summary, both regional EOFs, complemented by data from four other lake systems in
456 southeastern Australia, indicate that between 500-200 cal B.P. south-eastern Australia was
457 characterised by an increased moisture balance, following a prior period of reduced moisture
458 balance, supporting the interpretation by Barr et al. (2014). However the timing and pattern
459 of change differs between sites, a possible consequence of chronological uncertainty, but also
460 possibly reflecting differences in the hydrological sensitivity of each system to climate
461 forcing. A number of factors influence the hydrological sensitivity of lakes, however large
462 lakes, or those fed by groundwater, are less likely to respond rapidly to short term climate
463 changes compared to more shallow, isolated lake basins, resulting in markedly lagged
464 patterns of change between records (Jones et al., 2001; Wigdahl et al., 2014). Differences in
465 sediment accumulation rate, chemical composition and lake bathymetry are also likely to have
466 an effect. The limitations of regional EOFs in light of differences in the sensitivity, temporal
467 resolution and chronological precision between lakes are highlighted by the records from
468 Lake Elingamite and Rebecca Lagoon, both of which indicate a shorter period of wetter
469 conditions between ~900-650 cal B.P. which is not manifest in either regional EOF (Figure

6b). As discussed above, the causes and mechanisms behind these inconsistencies is an interesting subject for future research.

The pattern depicted in regional EOF 2 is comparable to reconstructed air temperature changes over Australasia, with lower temperatures and a reduction in the magnitude of inter-decadal variance, from ~500 cal B.P. onwards (Figure 6b; PAGES 2k Consortium, 2013). Rainfall variability in southeastern Australia is subject to widespread influences, including changes in the Southern Annular Mode and Indian Ocean Dipole (Hendon et al., 2007; Risbey et al., 2009; Ummenhofer et al., 2009; Vance et al., 2013). However, it is interesting to note that both regional EOFs appear to exhibit similar patterns to the frequency of El Niño events recorded in the sediments of Lago Pallcacocha, Equador, whereby dry conditions in southeastern Australia correspond to more frequent El Niño events (Figure 6b; Moy et al., 2002). The regional pattern depicted in Figure 6 contrasts with opposite trends recorded in saline lakes in the Wimmera region of northern Victoria (Kemp et al., 2012) and an increase in dust transport from the Murray Darling Basin (Marx et al., 2011). In addition, exposed shorelines from the playa Lake Callabonna, South Australia, suggest a lake high stand occurred during the Northern Hemisphere's Medieval Climate Anomaly at a time when Western Victorian lakes were relatively dry (Cohen et al., 2012). Such spatial heterogeneity points towards a complex pattern of surface hydrology and seasonality across southeastern Australia, for which further data generation and synthesis are required for a more complete understanding (Gouramanis et al., 2013).

Conclusion

Palaeoclimate research is moving away from the traditional single site approach, towards utilising the increasing number of datasets, arranged in space, to pick apart the primary features of climate and environmental change. However, identifying regionally coherent patterns amongst multiple environmental timeseries can be challenging, particularly since

such records are usually diverse, age uncertain, non-quantitative and multivariate. Performing prior site specific (local) ordination is one means of reducing such multivariate datasets to a limited number of representative variables, and here we demonstrate the potential of this approach using four diatom records from maar lakes in Western Victoria, Australia. We used detrended correspondence analysis to reduce the local (site-specific) diatom microfossil datasets, before applying principal components analysis to identify the regional (between-site) common patterns. Our analysis reveals coherent signals between all of the four records studied, suggesting that the lake ecosystems all varied in response to a common external forcing. Interestingly, the same patterns are not always manifest in the first DCA axis for each site, thus a similar approach based on single variables from each site might have overlooked such coherency. The common forcing most likely reflects regional hydroclimatic change, which have a marked effect on the hydrology of the studied lakes. There is therefore considerable potential for expanding this approach to identify widespread patterns of environmental and climate change in Australia and beyond.

Acknowledgements

The authors would like to thank Gavin Simpson, Peter Minchin and Bob Clarke for their advice on dimension reduction techniques in ecology, Maarten Blaauw for his advice on age-depth modelling and Kevin Anchukaitis and Jessica Tierney for sharing their Matlab code for Monte Carlo Empirical Orthogonal Functions. John Tibby's comments on an earlier version of this manuscript were much appreciated. This research was funded by two Collaborative Research Network (CRN) fellowships to JJT and KM, an Australian Postgraduate Award (APA) and an Australian Institute of Nuclear Science and Engineering (AINSE) postgraduate research award (AINSTU0104) to CB and an Australian Research Council Discovery Early Career Research Award (DECRA) to KS.

522

523

524 **References**

525

526 Anchukaitis, K.J., Tierney, J.E., 2012. Identifying coherent spatiotemporal modes in time-
527 uncertain proxy palaeoclimate records. Climate Dynamics DOI: 10.1007/s00382-012-1483-0.

528 Anderson, N.J., Liversidge, A.C., McGowan, S., Jones, M.D., 2012. Lake and catchment
529 response to Holocene environmental change: spatial variability along a climate gradient in
530 southwest Greenland. Journal of Paleolimnology 48, 209-222.

531 Barr, C., 2010. Droughts and flooding rains: a fine resolution reconstruction of climatic
532 variability in western Victoria, Australia, over the last 1500 years. University of Adelaide,
533 Australia.

534 Barr, C., Tibby, J., Gell, P.G., Tyler, J.J., Zawadzki, A., Jacobsen, G.E., 2014. Climate
535 variability in south-eastern Australia over the last 1500 years inferred from the high-
536 resolution diatom records of two crater lakes Quat. Sci. Rev. 95, 115-131.

537 Battarbee, R.W., 2000. Palaeolimnological approaches to climate change, with special regard
538 to the biological record. Quat. Sci. Rev. 19, 107-124.

539 Bennett, K.D., 1996. Determination of the number of zones in a biostratigraphical sequence.
540 New Phytologist 132, 155-170.

541 Birks, H.J.B., 2007. Estimating the amount of compositional change in Late-Quaternary
542 pollen-stratigraphical data. Veg. Hist. Archaeobot. 16, 197-202.

543 Birks, H.J.B., Lotter, A.F., Juggins, S., Smol, J.P., 2012. Tracking Environmental Change
544 Using Lake Sediments. Volume 5: Data Handling and Numerical Techniques. Springer,
545 Dordrecht.

546 Blaauw, M., 2010. Methods and code for 'classical' age-modelling of radiocarbon sequences.
547 Quaternary Geochronology 5, 512-518.

548 Blaauw, M., 2012. Out of tune: the dangers of aligning proxy archives. Quat. Sci. Rev. 36,
549 38-49.

550 Blaauw, M., Christen, A.J., 2011. Flexible Paleoclimate Age-Depth Models Using an
551 Autoregressive Gamma Process. Bayesian Analysis 6, 457-474.

552 Bowler, J.M., Hamada, T., 1971. Late Quaternary stratigraphy and radiocarbon chronology of
553 water level fluctuations in Lake Keilambete, Victoria. Nature 232, 330-&.

554 Bronk Ramsey, C., 2008. Deposition models for radiocarbon dating. Quat. Sci. Rev. 27, 42-
555 60.

556 Chen, G., Dalton, C., Taylor, D., 2010. Cladocera as indicators of trophic state in Irish lakes.
557 JOURNAL OF PALEOLIMNOLOGY 44, 465-481.

558 Clark, P.U., Dyke, A.S., Shakun, J.D., Carlson, A.E., Clark, J., Wohlfarth, B., Mitrovica, J.X.,
559 Hostetler, S.W., McCabe, A.M., 2009. The Last Glacial Maximum. Science 325, 710-714.

560 Clark, P.U., Hostetler, S.W., Pisias, N.G., Schmittner, A., Meissner, K.J., 2007. Mechanisms
561 for an ~7-kyr Climate and Sea-Level Oscillation During Marine Isotope Stage 3, Ocean
562 Circulation: Mechanisms and Impacts. American Geophysical Union, pp. 209-246.

563 Clark, P.U., Shakun, J.D., Baker, P.A., Bartlein, P.J., Brewer, S., Brook, E., Carlson, A.E.,
564 Cheng, H., Kaufman, D.S., Liu, Z., Marchitto, T.M., Mix, A.C., Morrill, C., Otto-Bliesner,
565 B.L., Pahnke, K., Russell, J.M., Whitlock, C., Adkins, J.F., Blois, J.L., Clark, J., Colman,
566 S.M., Curry, W.B., Flower, B.P., He, F., Johnson, T.C., Lynch-Stieglitz, J., Markgraf, V.,
567 McManus, J.F., Mitrovica, J.X., Moreno, P.I., Williams, J.W., 2012. Global climate evolution
568 during the last deglaciation. Proceedings of the National Academy of Sciences of the United
569 States of America 109, E1134-E1142.

570 Clarke, K.R., Warwick, R.M., 2001. Change in marine communities: an approach to statistical
571 analysis and interpretation, 2nd edition. . PRIMER-E, Plymouth, U.K.

572 Cohen, T.J., Nanson, G.C., Jansen, J.D., Gliganic, L.A., May, J.-H., Larsen, J.R., Goodwin,
573 I.D., Browning, S., Price, D.M., 2012. A pluvial episode identified in arid Australia during the
574 Medieval Climatic Anomaly. Quat. Sci. Rev. 56, 167-171.

575 Cook, E.R., Buckley, B.M., D'Arrigo, R.D., Peterson, M.J., 2000. Warm-season temperatures
576 since 1600 BC reconstructed from Tasmanian tree rings and their relationship to large-scale
577 sea surface temperature anomalies. Climate Dynamics 16, 79-91.

578 Davidson, T.A., Reid, M.A., Sayer, C.D., Chilcott, S., 2013. Palaeolimnological records of
579 shallow lake biodiversity change: exploring the merits of single versus multi-proxy
580 approaches. JOURNAL OF PALEOLIMNOLOGY 49, 431-446.

581 Davidson, T.A., Sayer, C.D., Perrow, M.R., Bramm, M., Jeppesen, E., 2007. Are the controls
582 of species composition similar for contemporary and sub-fossil cladoceran assemblages? A
583 study of 39 shallow lakes of contrasting trophic status. JOURNAL OF PALEOLIMNOLOGY
584 38, 117-134.

585 De Deckker, P., 1982. Holocene ostracods, other invertebrates and fish remains from cores of
586 four maar lakes in Southeastern Australia. Proceedings of the Royal Society of Victoria 94,
587 183-220.

588 Dodson, J.R., De Salis, T., Myers, C.A., Sharp, A.J., 1994. A thousand years of
589 environmental change and human impact in the alpine zone at Mt. Kosciusko, New South
590 Wales. Australian Geographer 25, 77-87.

591 Emile-Geay, J., Tingley, M., 2014 - in press. Inferring climate variability from nonlinear
592 proxies. Application to paleo-ENSO studies. Paleoceanography.

593 Engstrom, D.R., Fritz, S.C., Almendinger, J.E., Juggins, S., 2000. Chemical and biological
594 trends during lake evolution in recently deglaciated terrain. Nature 408, 161-166.

595 Faith, D.P., Minchin, P.R., Belbin, L., 1987. Compositional dissimilarity as a robust measure
596 of ecological distance. Plant Ecology 69, 57-68.

597 Gouramanis, C., De Deckker, P., Switzer, A.D., Wilkins, D., 2013. Cross-continent
598 comparison of high-resolution Holocene climate records from southern Australia -
599 Deciphering the impacts of far-field teleconnections. Earth-Science Reviews 121, 55-72.

600 Gouramanis, C., Wilkins, D., De Deckker, P., 2010. 6000 years of environmental changes
601 recorded in Blue Lake, South Australia, based on ostracod ecology and valve chemistry.
602 Palaeogeography Palaeoclimatology Palaeoecology 297, 223-237.

603 Greenacre, M.J., 1984. Theory and applications of correspondence analysis. Academic Press,
604 London, U.K.

605 Haig, J., Nott, J., Reichart, G.-J., 2014. Australian tropical cyclone activity lower than at any
606 time over the past 550-1,500 years. Nature 505, 667-671.

607 Hendon, H.H., Thompson, D.W.J., Wheeler, M.C., 2007. Australian rainfall and surface
608 temperature variations associated with the Southern Hemisphere annular mode. Journal of
609 Climate 20, 2452-2467.

610 Hill, M.O., 1979. DECORANA - a FORTRAN program for detrended correspondence
611 analysis and reciprocal averaging. Cornell University, Ithaca, New York.

612 Hill, M.O., Gauch, H.G., 1980. Detrended correspondence analysis: an improved ordination
613 technique. Vegetatio 42, 47-59.

614 Hogg, A.G., Hua, Q., Blackwell, P.G., Niu, M., Buck, C.E., Guilderson, T.P., Heaton, T.J.,
615 Palmer, J.G., Reimer, P.J., Reimer, R.W., Turney, C.S.M., Zimmerman, S.R.H., 2013.
616 SHCAL13 Southern Hemisphere Calibration, 0-50,000 years cal BP. Radiocarbon 55, 1889-
617 1903.

618 Jones, R.N., McMahon, T., Bowler, J.M., 2001. Modelling historical lake levels and recent
619 climate change at three closed lakes, Western Victoria, Australia (c.1840-1990). Journal of
620 Hydrology 246, 159-180.

621 Jongman, R.H.G., ter Braak, C.J.F., van Tongeren, O.F.R., 1987. Data analysis in community
622 and landscape ecology. Pudoc Wageningen.

623 Juggins, S., 2013. Quantitative reconstructions in palaeolimnology: new paradigm or sick
624 science? Quat. Sci. Rev. 64, 20-32.

625 Kemp, J., Radke, L.C., Olley, J., Juggins, S., De Deckker, P., 2012. Holocene lake salinity
626 changes in the Wimmera, southeastern Australia, provide evidence for millennial-scale
627 climate variability. Quaternary Research 77, 65-76.

628 Kruskal, J.B., 1967. Nonmetric multidimensional scaling: a numerical method. Psychometrika
629 29, 115-129.

630 Leahy, P., Robinson, D., Pattern, R., Kramer, A., 2010. Lakes in the Western District of
631 Victoria and Climate Change, EPA Scientific Report, EPA Victoria, p. 61.

632 Legendre, P., Gallagher, E.D., 2001. Ecologically meaningful transformations for ordination
633 of species data. Oecologia 129, 271-280.

634 Legendre, P., Legendre, L.F.J., 1998. Numerical Ecology, Second English Edition. Elsevier,
635 Amsterdam.

636 Mann, M.E., Bradley, R.S., Hughes, M.K., 1998. Global-scale temperature patterns and
637 climate forcing over the past six centuries. Nature 392, 779-787.

638 Marx, S.K., Kamber, B.S., McGowan, H.A., Denholm, J., 2011. Holocene dust deposition
639 rates in Australia's Murray-Darling Basin record the interplay between aridity and the position
640 of the mid-latitude westerlies. Quat. Sci. Rev. 30, 3290-3305.

641 Mills, K., Gell, P.A., Kershaw, A.P., 2013. The recent Victorian drought and its impact.
642 Without precedent?, Rural Industries Research and Develpment Corporation, Barton, ACT.

643 Mills, K., Ryves, D.B., Anderson, N.J., Bryant, C., Tyler, J.J., 2014. Expressions of climate
644 perturbations in western Ugandan crater lake sediment records during the last 1000 yr
645 Climates of the Past, DOI: 10.5194/cpd-5199-5183-2013.

646 Minchin, P.R., 1987. An Evaluation of the Relative Robustness of Techniques for Ecological
647 Ordination. Vegetatio 69, 89-107.

648 Mooney, S., 1997. A fine-resolution paleoclimatic reconstruction of the last 2000 years, from
649 Lake Keilambete, southeastern Australia. Holocene 7, 139-149.

650 Moy, C.M., Seltzer, G.O., Rodbell, D.T., Anderson, D.M., 2002. Variability of El
651 Nino/Southern Oscillation activity at millennial timescales during the Holocene epoch. Nature
652 420, 162-165.

653 Neukom, R., Gergis, J., 2012. Southern Hemisphere high-resolution palaeoclimate records of
654 the last 2000 years. Holocene 22, 501-524.

655 Nicholson, S.E., Nash, D.J., Chase, B.M., Grab, S.W., Shanahan, T.M., Verschuren, D.,
656 Asrat, A., Lezine, A.-M., Umer, M., 2013. Temperature variability over Africa during the last
657 2000 years. The Holocene 0 !!!!!, 1-10.

658 Oksanen, J., Kindt, R., Legendre, P., O'Hara, B., Simpson, G.L., Solymos, P., Stevens,
659 M.H.H., Wagner, H., 2008. Vegan: community ecology package. R package version 1.15-1.

660 PAGES 2k Consortium, 2013. Continental-scale temperature variability during the past two
661 millennia. Nature Geoscience 6, 339-346.

662 Peres-Neto, P.R., Jackson, D.A., 2001. How well do multivariate data sets match? The
663 advantages of a Procrustean superimposition approach over the Mantel test. Oecologia 129,
664 169-178.

665 Risbey, J.S., Pook, M.J., McIntosh, P.C., Wheeler, M.C., Hendon, H.H., 2009. On the Remote
666 Drivers of Rainfall Variability in Australia. Monthly Weather Review 137, 3233-3253.

667 Saunders, K.M., Grosjean, M., Hodgson, D.A., 2013. A 950-year temperature reconstruction
668 from Duckhole Lake, southern Tasmania, Australia. The Holocene 23, 771-783.

669 Saunders, K.M., Kamenik, C., Hodgson, D.A., Hunziker, S., Siffert, L., Fischer, D., Fujak,
670 M., Gibson, J.A.E., Grosjean, M., 2012. Late Holocene changes in precipitation in northwest
671 Tasmania and their potential links to shifts in the Southern Hemisphere westerly winds.
672 Global and Planetary Change 92-93, 82-91.

673 Shakun, J.D., Carlson, A.E., 2010. A global perspective on Last Glacial Maximum to
674 Holocene climate change. Quat. Sci. Rev. 29, 1801-1816.

675 Shakun, J.D., Clark, P.U., He, F., Marcott, S.A., Mix, A.C., Liu, Z., Otto-Bliesner, B.,
676 Schmittner, A., Bard, E., 2012. Global warming preceded by increasing carbon dioxide
677 concentrations during the last deglaciation. Nature 484, 49-+.

678 Simpson, G.L., Birks, H.J.B., 2012. Statistical Learning in Palaeolimnology, in: Birks, H.J.B.,
679 Lotter, A.F., Juggins, S., Smol, J.P. (Eds.), Data Handling and Numerical Techniques.
680 Springer, Dordrecht, pp. 249-327.

681 Smith, T.M., Reynolds, R.W., Livezey, R.E., Stokes, D.C., 1996. Reconstruction of Historical
682 Sea Surface Temperatures Using Empirical Orthogonal Functions. Journal of Climate 9,
683 1403-1420.

684 Smol, J.P., Wolfe, A.P., Birks, H.J.B., Douglas, M.S.V., Jones, V.J., Korhola, A., Pienitz, R.,
685 Ruhland, K., Sorvari, S., Antoniades, D., Brooks, S.J., Fallu, M.A., Hughes, M., Keatley,
686 B.E., Laing, T.E., Michelutti, N., Nazarova, L., Nyman, M., Paterson, A.M., Perren, B.,
687 Quinlan, R., Rautio, M., Saulnier-Talbot, E., Siitoneni, S., Solovieva, N., Weckstrom, J.,
688 2005. Climate-driven regime shifts in the biological communities of arctic lakes. Proceedings
689 of the National Academy of Sciences of the United States of America 102, 4397-4402.

690 Tibby, J., Penny, T., Leahy, P., Kershaw, A.P., 2012. Vegetation and water quality responses
691 to Holocene climate variability in Lake Purrumbete, western Victoria, in: Haberle, S.G.,
692 David, I. (Eds.), Peopled Landscapes: Archaeological and Biogeographic Approaches to
693 ANU E-Press, Canberra, pp. 359-376.

694 Tibby, J., Tiller, D., 2007. Climate-water quality relationships in three Western Victorian
695 (Australia) lakes 1984-2000. Hydrobiologia 591, 219-234.

696 Tierney, J.E., Smerdon, J.E., Anchukaitis, K.J., Seager, R., 2013. Multidecadal variability in
697 East African hydroclimate controlled by the Indian Ocean. Nature 493, 389-392.

698 Ummenhofer, C.C., England, M.H., McIntosh, P.C., Meyers, G.A., Pook, M.J., Risbey, J.S.,
699 Gupta, A.S., Taschetto, A.S., 2009. What causes southeast Australia's worst droughts?
700 Geophysical Research Letters 36.

701 Vance, T., van Ommen, T.D., Curran, M.A.J., Plummer, C.T., Moy, A.D., 2013. A Millennial
702 Proxy Record of ENSO nad Eastern Australian Rainfall from the Law Dome Ice Core,
703 Antarctica. Journal of Climate 26, 710-725.

704 Wang, L., Lu, H., Liu, J., Gu, Z., Mingram, J., Chu, G., Li, J., Rioual, P., Negendank, J.F.W.,
705 Han, J., Liu, T., 2008. Diatom-based inference of variations in the strength of Asian winter
706 monsoon winds between 17,500 and 6,000 calendar years B.P. Journal of Geophysical
707 Research 133, D21101.

708 Weare, B.C., Navato, A.R., Newell, R.E., 1976. Empirical orthogonal analysis of Pacific sea
709 surface temperatures. Journal of Physical Oceanography 6, 671-678.

710 Wigdahl, C.R., Saros, J.E., Fritz, S.C., Stone, J.R., Engstrom, D.R., 2014. The influence of
711 basin morphometry on the regional coherence of patterns of diatom-inferred salinity in lakes
712 of the northern Great Plains (USA). The Holocene, DOI: 10.1177/0959683614523154

713 Wilkins, D., De Deckker, P., Fifield, L.K., Gouramanis, C., Olley, J.M., 2012. Comparative
714 optical and radiocarbon dating of laminated Holocene sediments in two maar lakes: Lake
715 Keilambete and Lake Gnotuk, south-western Victoria, Australia. Quaternary Geochronology
716 9, 3-15.

717 Wilkins, D., Gouramanis, C., De Deckker, P., Fifield, L.K., Olley, J.M., 2013. Holocene lake
718 level fluctuations in Lake Keilambete and Lake Gnotuk, south-western Victoria, Australia.
719 Holocene in press.

720 Wischnewski, J., Kramer, A., Kong, Z., Mackay, A.W., Simpson, G.L., Mischke, S.,
721 Herzschuh, U., 2011a. Terrestrial and aquatic responses to climate change and human impact
722 on the southeastern Tibetan Plateau during the past two centuries. Global Change Biology 17,
723 3376-3391.

724 Wischnewski, J., Mischke, S., Wang, Y., Herzschuh, U., 2011b. Reconstructing climate
725 variability on the northeastern Tibetan Plateau since the last Lateglacial - a multi-proxy, dual-
726 site approach comparing terrestrial and aquatic signals. Quat. Sci. Rev. 30, 82-97.
727

728

729

730

731

732

733 **Table Captions**

734 Table 1: List of diatom taxa occurring as >2.5% of any sample from each site and associated
735 loading upon DCA axes 1-3.

736

737

738 **Figure Captions**

739 Figure 1: Location of lake sites in western Victoria, Australia. The lake sites studied are
740 written in bold, italic font and underlined. Other lakes in the region are written in italics, and
741 nearby towns are written in bold font. In subset B, major cities in the region are written in
742 lower case italics. Sea is shaded grey in all figures.

743

744 Figure 2: Age-depth plots for each site. Blue and green histograms depict probability
745 distribution of calibrated radiocarbon and ^{210}Pb ages respectively. Dates excluded in the
746 original studies are not plotted. Gray shading indicates the 2sd deviation from the most likely
747 model, based on 10,000 iterations.

748

749 Figure 3: Detrended correspondence analysis (DCA) biplots for each site, depicting
750 association between samples (coloured points) and common diatom taxa. Diatom taxa were
751 screened as those with a maximum abundance ≥ 5% for all sites except Lake Surprise, where
752 the cutoff was ≥ 10%. The point colour depicts the weighted mean calibrated age of each
753 sample, as indicated in the legend. A quadratic trend surface is plotted in green, depicting the
754 association between samples and diatom inferred lake water conductivity (salinity), as taken
755 from the original data sources.

756

757 Figure 4: Time series of DCA axis scores for each site, with errors based upon 10,000
758 iterations within the bounds of each age model. Black lines = median timeseries, dark shading
759 = 90% confidence intervals and pale shading = 68% confidence intervals.

760

761 Figure 5: Screeplot of variance explained (inertia) vs. axis number for PCA analysis of all site
762 specific DCA scores. Solid black line = mean solution from 10,000 age iterations, solid grey
763 line = 1sd error and dashed grey line = 2sd error. Red line = broken stick model, used as a test
764 of axis significance (Bennett, 1996).

765

766 Figure 6: Time series of regional EOFs, based on PCA analysis of local DCA scores. Black
767 lines = median timeseries, dark shading = 90% confidence intervals and pale shading = 68%
768 confidence intervals.

769

770 Figure 7: Biplot depicting variable loading upon each EOF. Site is depicted in colour (see
771 legend inset), and site-specific DCA axis is indicated by the number of each point. Error bars
772 depict 2sd error.

773

774

775

776

777

778

779

780

FIGURES

Table 1

Lake Elinganite	DCA1	DCA2	DCA3
Psammothidium sacculum	-1.03	1.03	0.73
Achnanthidium minutissimum	-2.08	-1.18	-1.22
Amphora copulata	0.50	1.05	0.13
Caloneis silicula	0.78	1.57	-1.86
Cocconeis placentula	-0.38	2.02	1.46
Craticula cuspidata	-0.02	0.76	-0.19
Discoatella pseudostelligera	0.10	0.31	-0.62
Discostella stelligera	-0.36	-1.19	0.43
Cymbella naviculiformis	0.48	1.10	-0.42
Fragilaria capucina	-0.89	0.57	-0.14
Fragilaria crotonensis	-3.62	-0.98	0.34
Frankophiloa similoides	0.29	-0.62	-0.06
Navicula cryptocephala	1.70	-1.33	0.92
Navicula heimansioides	-2.14	0.89	0.30
Placoneis placentula	-0.80	1.45	-2.14
Sellaphora pupula	0.06	0.53	-0.33
Staurosira construens v. construens	2.40	0.08	0.52
Staurosira construens v. venter	2.43	-4.00	-4.15
Staurosira elliptica	2.25	2.02	1.42
Staurosirella pinnata	0.52	-0.78	0.68

Lake Purrumbete	DCA1	DCA2	DCA3
Discostella stelligera	-0.83	-1.21	-0.68
Sellaphora pupula	-0.33	-0.66	-1.22
Achnanthidium exiguum	0.22	-0.24	-0.46
Achnanthidium minutissimum	0.12	-2.01	-0.86
Discostella pseudostelligera	0.82	0.09	-0.41
Rhopalodia gibba	0.13	-0.92	0.76
Cymbella cistula	0.12	-0.52	0.21
Aulacoseira pusilla	0.82	0.72	-0.17
Amphora copulata	0.35	-0.05	-0.51
Cymbella minuta	-0.32	0.31	-0.24
Cocconeis placentula	0.13	-0.51	-0.14
Epithemia adnata	0.08	-0.01	-0.64
Navicula peregrina	-0.20	-0.56	-1.19
Staurosira construens	-0.13	0.52	0.20
Achnanthidium lanceolatum	0.32	0.24	0.12
Tabularia fasciculata	0.43	0.52	-0.11
Encyonema silesiacum	-3.50	2.95	-2.17
Staurosirella leptostauron	4.28	-0.91	2.51
Staurosira elliptica	0.38	0.08	0.41
Achnanthes curtissima	0.45	-0.14	0.95
Fragilaria subsalina	0.94	1.16	-0.52
Fragilaria sopotensis	-0.04	0.78	0.40
Staurosirella pinnata	-0.87	0.53	1.36

Lake Surprise	DCA1	DCA2	DCA3
Achnanthidium minutissimum	2.62	0.58	0.43
Amphora copulata	-1.49	-0.53	-0.73
Amphora pediculus	-1.35	-2.91	-0.95
Aulacoseira granulata	0.34	-0.57	3.39
Caloneis silicula	-0.51	-0.61	-0.78
Cocconeis placentula	0.33	0.63	0.24
Craticula accomoda	1.64	0.39	0.18
Cyclostephanos dubius	-0.90	1.55	1.66
Cyclostephanos tholiformis	-0.91	1.86	1.70
Cyclotella meneghiniana	-0.74	-0.85	-0.80
Discostella pseudostelligera	-0.22	-2.04	-1.07
Discostella stelligera	-0.08	-3.90	-1.41
Cymbella cistula	0.76	0.49	-0.20
Encyonopsis microcephala	2.48	0.56	0.23
Encyonopsis rutneri	2.40	0.31	0.67
Fragilaria polonica	-1.01	-0.81	-0.32
Fragilaria zeilleri	-0.39	-0.69	-0.26
Frankophila similioides	-1.47	-3.09	-0.85
Gomphonema affine	1.04	0.46	0.00
Gomphonema minutum	1.67	0.55	-0.28
Karayevia clevei	-2.29	-1.17	-0.90
Placoneis clementis	-1.21	-2.51	-0.71
Navicula cryptocephala	1.83	-0.93	-0.91
Navicula cryptotenella	0.40	0.15	-0.38
Navicula menisculus	1.43	-0.10	-0.75
Navicula peregrina	-1.26	-0.47	-0.77
Placoneis placentula	-1.94	-0.61	-1.07
Navicula veneta	1.31	0.86	1.86
Navicula viridula	-1.09	-1.19	-1.00
Nitzschia amphibia	0.82	0.11	0.33
Nitzschia gracilis	0.13	0.68	5.32
Nitzschia palea	2.15	0.84	-0.64
Nitzschia paleacea	1.02	1.39	-1.94
Opephora olsenii	-2.28	-1.24	-0.89
Sellaphora laevissima	-0.75	-0.19	-0.26
Sellaphora pupula	-0.21	-0.01	-0.35
Staurosira construens v. construens	2.65	-2.37	4.03
Staurosira elliptica	0.27	-1.21	0.69
Staurosirella leptostauron	-1.68	-0.43	-0.91
Staurosirella pinnata	1.06	-0.82	1.46
Stephanodiscus hantzschii	-0.96	2.09	1.25
Stephanodiscus parvus	-2.32	1.07	0.61
Synedra acus	0.91	0.64	-1.26
Tabularia fasciculata	-1.92	-1.67	-0.74

Lake Tower Hill	DCA1	DCA2	DCA3
Cocconeis placentula	-0.97	-0.50	0.30
Cymbella cistula	-0.36	-0.80	1.21
Nitzschia palea	-1.08	-2.29	-1.29
Encyonema silesiacum	-2.01	-0.53	1.57
Pinnuavis elegans	-1.06	2.54	1.22
Sellaphora pupula	0.94	0.66	-0.52
Amphora veneta	0.08	-0.54	-0.13
Navicella pusilla	-0.07	-0.96	-0.55
Tabularia fasciculata	-1.22	0.73	-0.14
Navicula veneta	-0.41	-0.73	0.13
Anomoeoneis sphaerophora	1.01	-0.42	0.88
Achnanthidium minutissimum	-1.29	0.60	0.50
Amphora copulata	0.82	-0.04	0.43
Cymbella affinis	1.44	-2.87	1.58
Diadesmis contenta	1.65	-2.92	3.63

806 Figure 1

807

808

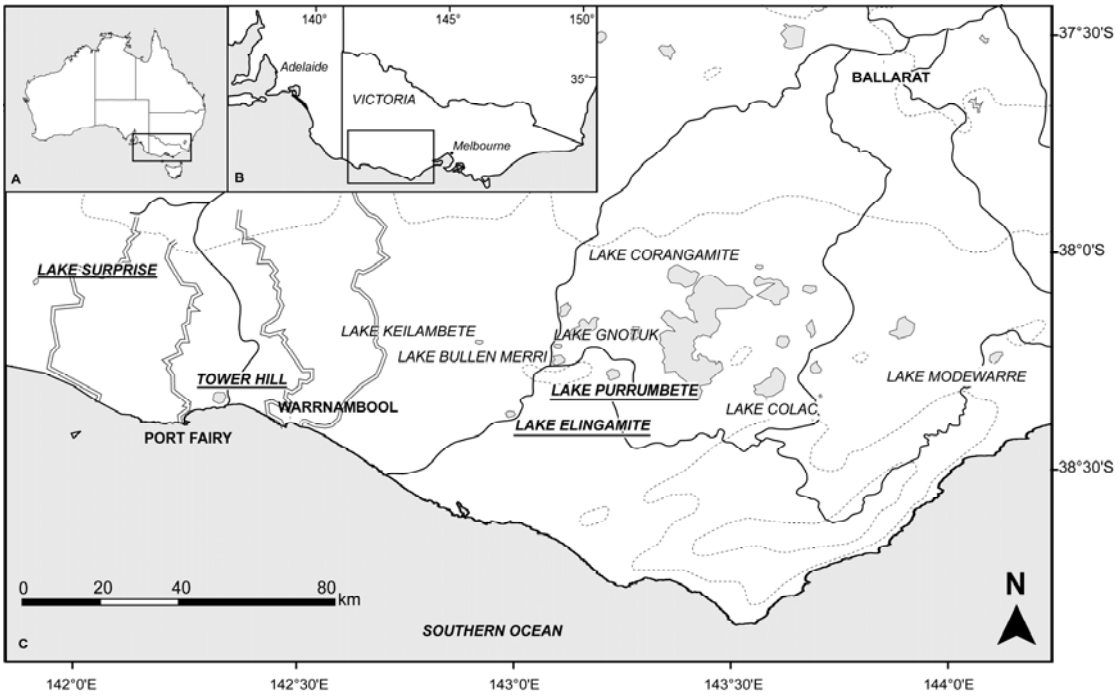

809

810

811

812

813

814

815

816

817

818

819

820

821

822 Figure 2

823

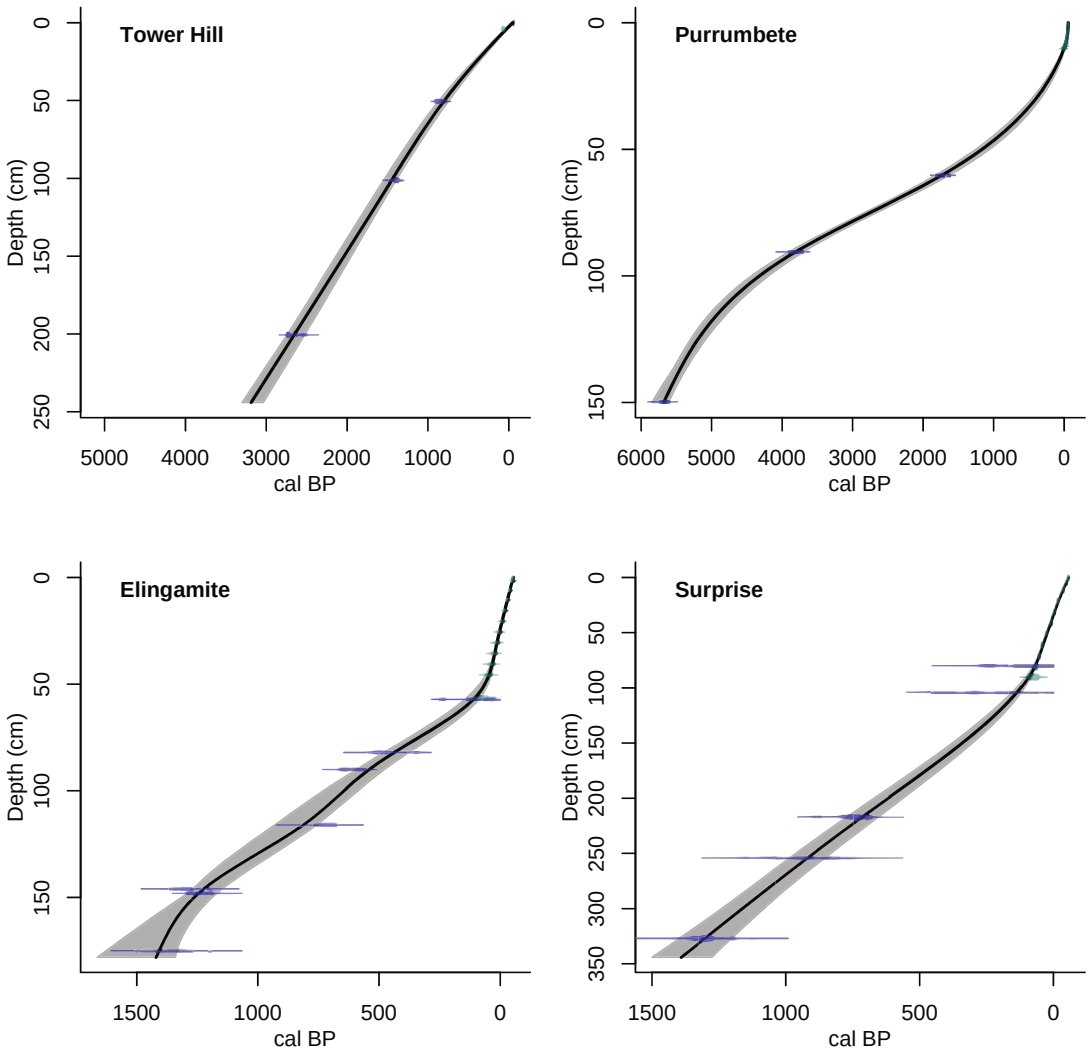

824

825

826

827

828

829

830

831

832

833 Figure 3

834

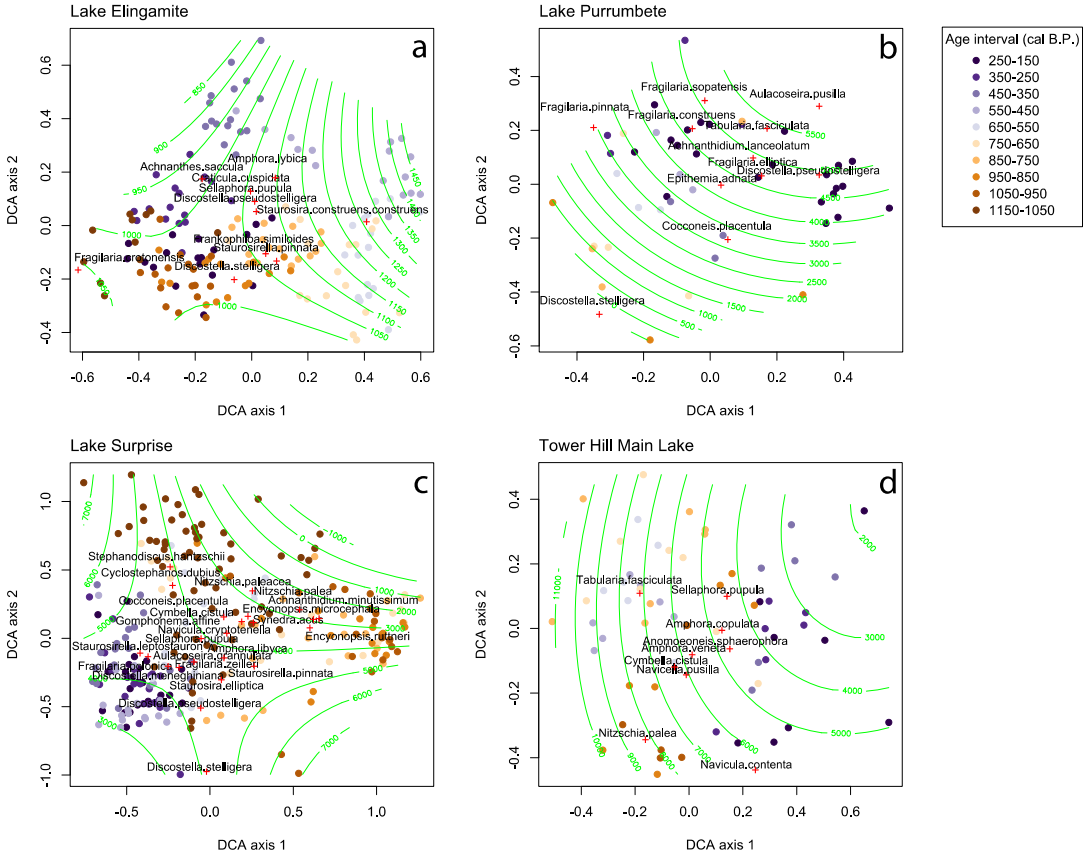

835

836 Figure 4

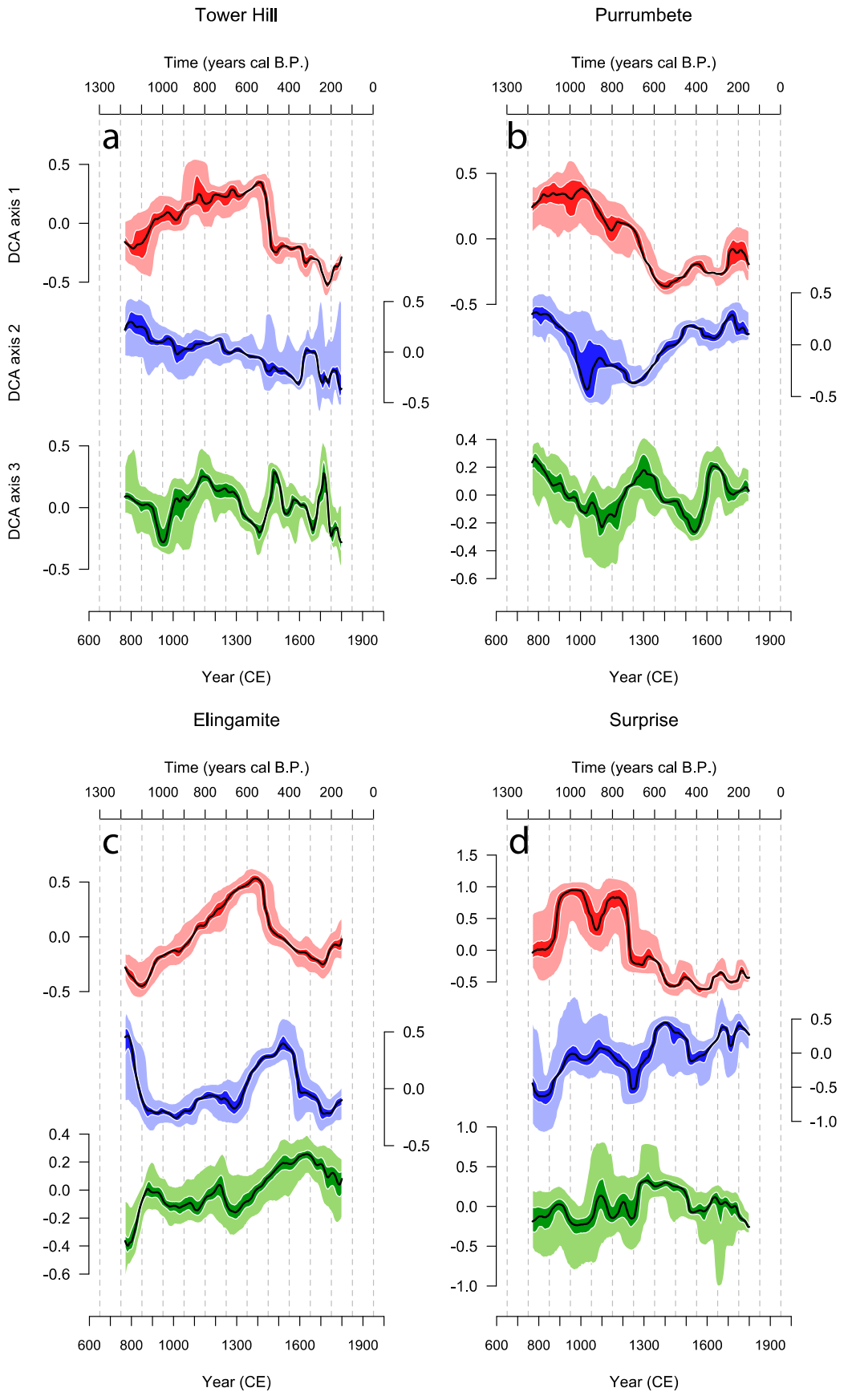

837

838 Figure 5

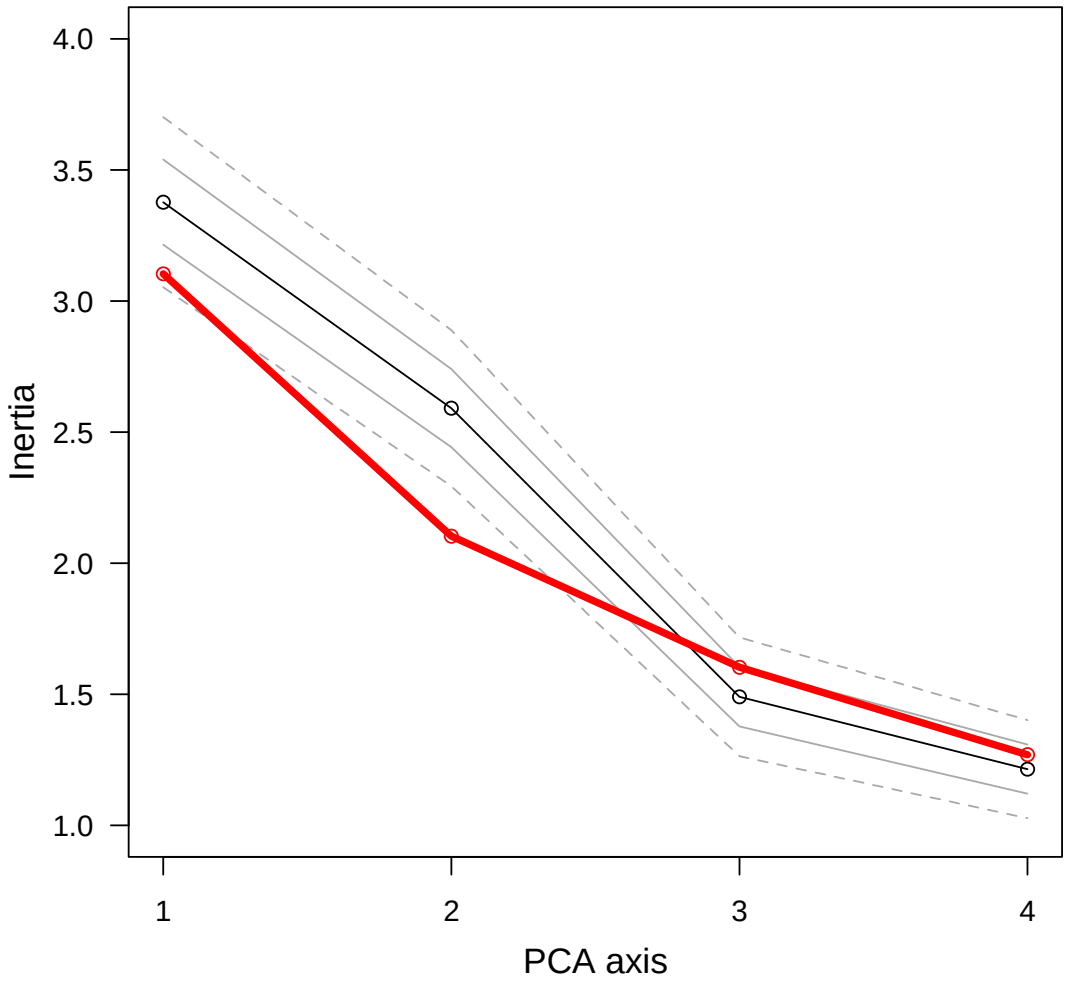

839

840

841

842

843

844

845

846

847 Figure 6

848

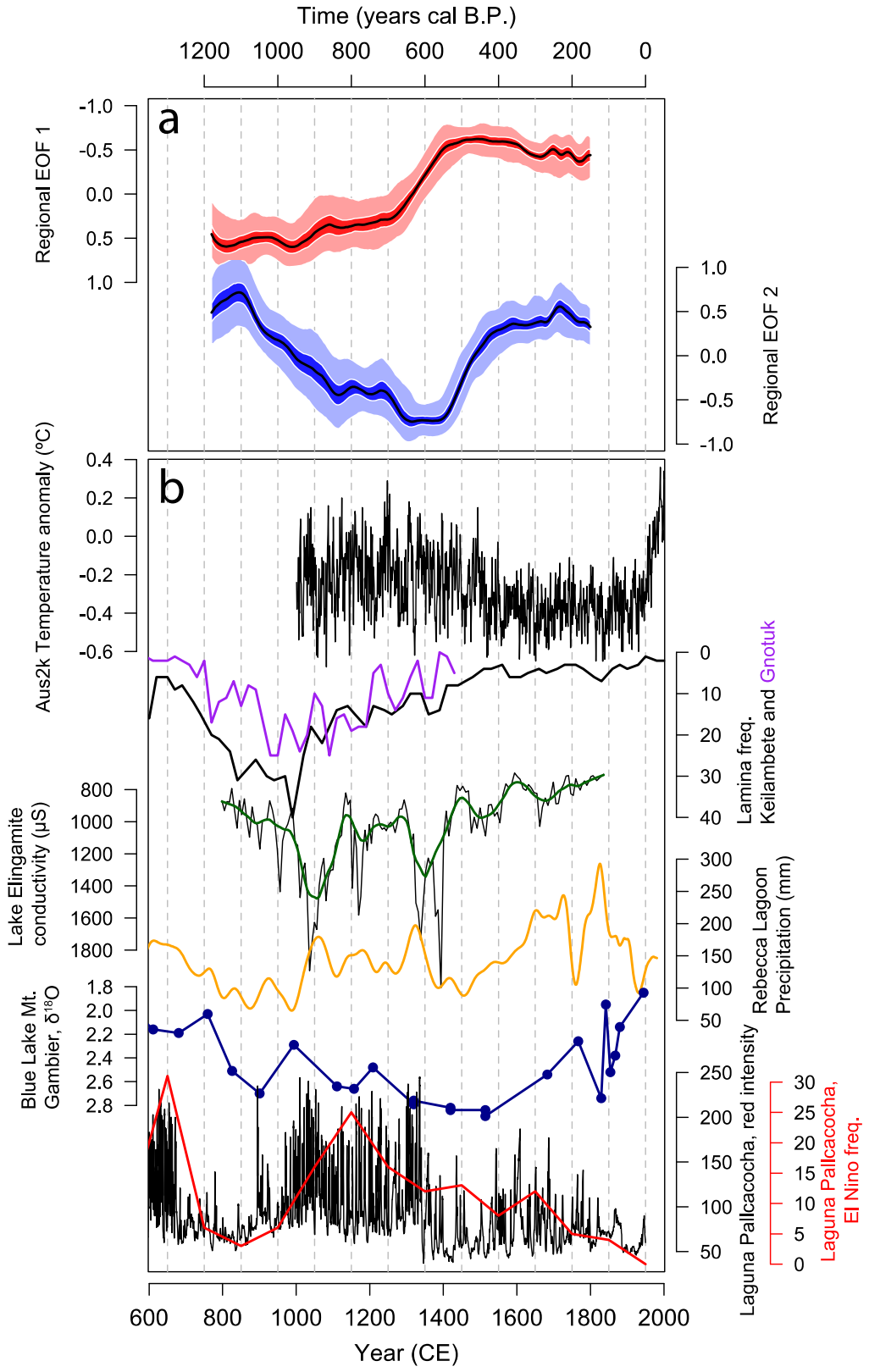

849

850 Figure 7

851

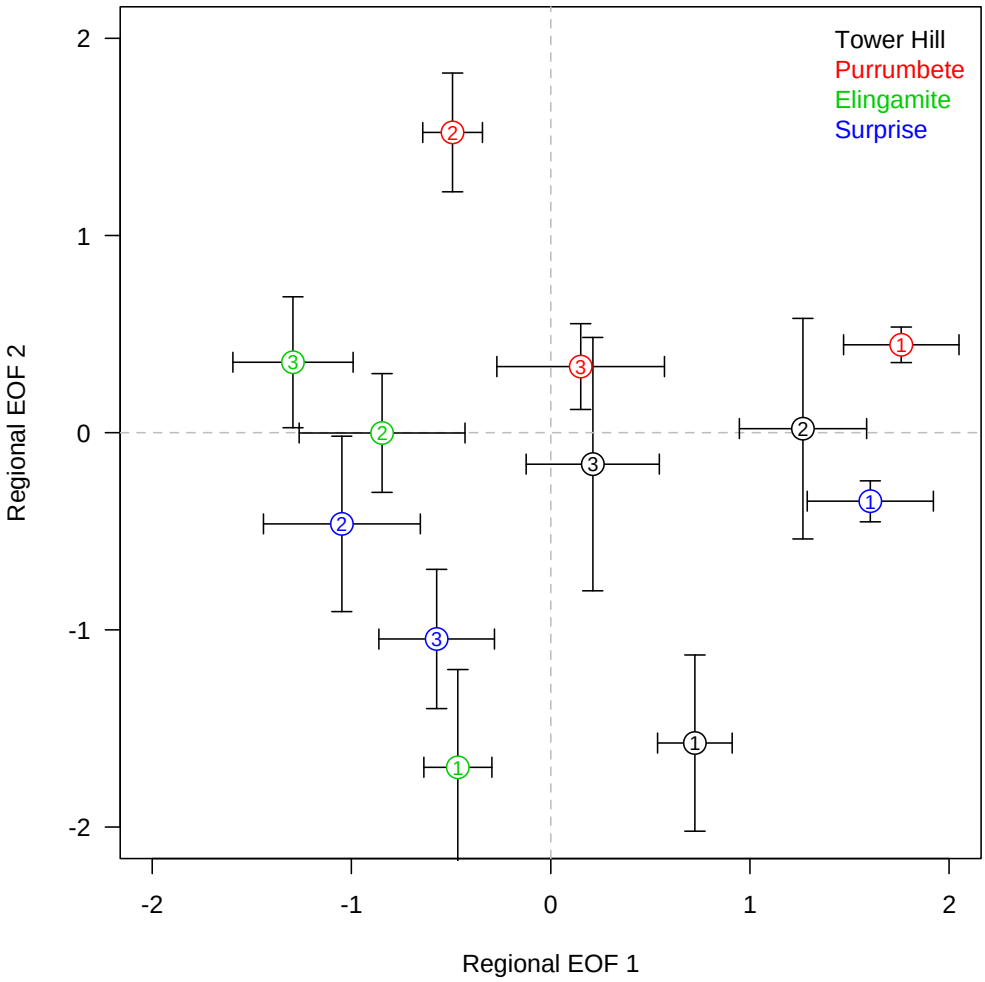

852

853

854

855